



**Fermi National Accelerator Laboratory**

**FERMILAB-Pub-98/090-E**

**E687**

**Observation of a Narrow State Decaying into  $\Xi_c^0 \pi^+$**

P.L. Frabetti et al.  
The E687 Collaboration

*Fermi National Accelerator Laboratory  
P.O. Box 500, Batavia, Illinois 60510*

March 1998

Submitted to *Physics Letters B*

# Observation of a Narrow State Decaying into $\Xi_c^0\pi^+$

E687 Collaboration

P.L. Frabetti

Dip. di Fisica dell'Università and INFN–Bologna, I-40126 Bologna, Italy

H.W.K. Cheung [a], J.P. Cumalat, C. Dallapiccola [b], J.F. Ginkel, W.E. Johns [c],

M.S. Nehring [d], E.W. Vaandering

University of Colorado, Boulder, CO 80309, USA

J.N. Butler, S. Cihangir, I. Gaines, P.H. Garbincius, L. Garren, S.A. Gourlay,

D.J. Harding, P. Kasper, A. Kreymer, P. Lebrun, S. Shukla, M. Vittone

Fermilab, Batavia, IL 60510, USA

S. Bianco, F.L. Fabbri, S. Sarwar, A. Zallo

Laboratori Nazionali di Frascati dell'INFN, I-00044 Frascati, Italy

C. Cawlfeld, R. Culbertson [e], R.W. Gardner [f], E. Gottschalk, R. Greene [g],

K. Park, A. Rahimi, J. Wiss

University of Illinois at Urbana–Champaign, Urbana, IL 61801, USA

G. Alimonti, G. Bellini, M. Boschini, D. Brambilla, B. Caccianiga, L. Cinquini [h],

M. Di Corato, P. Dini, M. Giammarchi, P. Inzani, F. Leveraro, S. Malvezzi,

D. Menasce, E. Meroni, L. Milazzo, L. Moroni, D. Pedrini, L. Perasso, F. Prelz,

A. Sala, S. Sala, D. Torretta

Dip. di Fisica dell'Università and INFN–Milano, I-20133 Milan, Italy

D. Buchholz, D. Claes [i], B. Gobbi, B. O'Reilly [h]

Northwestern University, Evanston, IL 60208, USA

J.M. Bishop, N.M. Cason, C.J. Kennedy [j], G.N. Kim [k], T.F. Lin, D.L. Pusejlic [j],

R.C. Ruchti, W.D. Shephard, J.A. Swiatek [l], Z.Y. Wu [m]

University of Notre Dame, Notre Dame, IN 46556, USA

V. Arena, G. Boca, G. Bonomi, C. Castoldi, G. Gianini, M. Merlo, S.P. Ratti,  
C. Riccardi, L. Viola, P. Vitulo

Dip. di Fisica Nucleare e Teorica dell'Università and INFN–Pavia, I-27100 Pavia, Italy

A. Lopez, L. Mendez, A. Mirles, E. Montiel, D. Olaya [h], E. Ramirez [h], C. Rivera,  
Y. Zhang [n]

University of Puerto Rico at Mayaguez, Puerto Rico

J.M. Link, V.S. Paolone [o], P.M. Yager

University of California–Davis, Davis, CA 95616, USA

J.R. Wilson

University of South Carolina, Columbia, SC 29208, USA

J. Gao, M. Hosack, P.D. Sheldon

Vanderbilt University, Nashville, TN 37235, USA

F. Davenport

University of North Carolina–Asheville, Asheville, NC 28804, USA

K. Cho, K. Danyo[p], T. Handler

University of Tennessee, Knoxville, TN 37996, USA

B.G. Cheon [q], Y.S. Chung, J.S. Kang, K.Y. Kim, K.B. Lee, S.S. Myung

Korea University, Seoul 136–701, Korea

## Abstract

We report the observation of the  $\Xi_c^{*+}$  state decaying into  $\Xi_c^0\pi^+$  with  $\Xi_c^0 \rightarrow \Lambda\bar{K}^0\pi^+\pi^-$  or  $\Lambda K^-\pi^+\pi^+\pi^-$ . We have observed  $47 \pm 11$  candidate events for the  $\Xi_c^{*+}$  state and measured its mass to be  $177.1 \pm 0.5 \pm 1.1$  MeV/ $c^2$  above the  $\Xi_c^0$  mass. We have also measured the  $\Xi_c^0$  mass to be  $2470.0 \pm 2.8 \pm 2.6$  MeV/ $c^2$ .

PACS: 14.20.Lq

Charm spectroscopy has provided important constraints for various models based on QCD and lattice gauge calculations. The heavy charm quark mass allows meaningful tests of these models to be made. These tests have been limited mainly to  $c\bar{c}$  bound states and charmed mesons due to the comparatively low production rate of charmed baryons. Excited charmed baryons, the topic of this paper, also provide rich information on the hadronic structure and on the forces governing that structure.

In the ground state isodoublet of charmed strange baryons, the  $\Xi_c^+$  and  $\Xi_c^0$ , the two light quarks are in a spin-singlet configuration. The lowest excited states are expected to be the  $J^P = \frac{1}{2}^+ \Xi_c'$  states and the  $J^P = \frac{3}{2}^+ \Xi_c^*$  states, in which the two light quarks are in a spin-triplet configuration. The very next higher excited state is believed to be an orbitally excited state, that is, in which the two light quarks are in spin-singlet configuration but the diquark has an orbital angular momentum,  $L = 1$ , with respect to the charm quark. Theoretical models[1] have predicted the mass of the  $\Xi_c'$  state to be below the threshold for the decay to  $\Xi_c\pi$ . If this is the case, the  $\Xi_c'$  must decay radiatively to the ground state through an electromagnetic dipole transition. The  $\Xi_c^*$  state is expected to occur in the mass range 2640–2690 MeV/ $c^2$ , which is massive enough to decay to the ground state by emitting a pion. The lowest orbitally excited state is predicted to occur at around 2760 MeV/ $c^2$  or a higher mass.

In recent years, there has been some progress in the charmed strange baryon spectroscopy. The WA89 collaboration at CERN presented preliminary evidence of the decay  $\Xi_c'^+ \rightarrow \Xi_c^+ \gamma$ , at a mass difference of about 95 MeV/ $c^2$  above the  $\Xi_c^+$  mass[2]. The CLEO collaboration recently presented evidence of the decay  $\Xi_c'^{+,0} \rightarrow \Xi_c^{+,0} \gamma$  and measured the preliminary mass differences  $M(\Xi_c^+ \gamma) - M(\Xi_c^+)$  and  $M(\Xi_c^0 \gamma) - M(\Xi_c^0)$  to be  $107.8 \pm 1.7 \pm 2.5$  MeV/ $c^2$  and  $107.0 \pm 1.4 \pm 2.5$  MeV/ $c^2$ , respectively[3]. The CLEO collaboration also reported evidence of two narrow states decaying into  $\Xi_c\pi$  and associated them with the  $\Xi_c^*$  states. They reported the two mass differences:  $M(\Xi_c^+ \pi^-) - M(\Xi_c^+) = 178.2 \pm 0.5 \pm 1.0$  MeV/ $c^2$  [4] and  $M(\Xi_c^0 \pi^+) - M(\Xi_c^0) = 174.3 \pm$

$0.5 \pm 1.0 \text{ MeV}/c^2$  [5]. More recently, the same collaboration claimed an observation of an orbitally excited state, the  $J^P = \frac{3}{2}^- \Xi_{c1}^+$  state with  $L = 1$ , of the  $\Xi_c^+$  baryon, which decays into  $\Xi_c^{*0}\pi^+$  followed by the decay  $\Xi_c^{*0} \rightarrow \Xi_c^+\pi^-$ . They measured the mass difference  $M(\Xi_c^+\pi^+\pi^-) - M(\Xi_c^+)$  to be  $349.4 \pm 0.7 \pm 1.0 \text{ MeV}/c^2$  [6].

This letter presents evidence of the photoproduction of the  $\Xi_c^{*+}$  state decaying into  $\Xi_c^0\pi^+$ , where the  $\Xi_c^0$  is reconstructed through its decays to  $\Lambda\bar{K}^0\pi^+\pi^-$  or  $\Lambda K^-\pi^+\pi^+\pi^-$  (throughout the paper, whenever a state is mentioned the charge conjugate state is implied) which have not been observed previously. We also report a new measurement of the  $\Xi_c^0$  mass based on combining these two decay modes with the  $\Xi^-\pi^+$  decay mode reported previously[7].

The data for this analysis were collected by the high energy photoproduction experiment E687 at Fermilab during the 1990–91 fixed target run. Charmed hadrons were produced by the interaction of a photon beam with mean momentum about 220 GeV/ $c$  on a 4 cm long beryllium target. The charm decay products were detected by a large aperture spectrometer which is described in detail elsewhere[8]. This analysis made use of information from the charged particle tracking system and the Čerenkov counters for particle identification. The tracking system consisted of a high resolution silicon microvertex detector (SSD), five stations of multi-wire proportional chambers (PWC's), and two analyzing magnets operated with opposite polarity.

We first reconstructed the  $\Xi_c^0$  candidate via its decay into  $\Lambda\bar{K}^0\pi^+\pi^-$  or  $\Lambda K^-\pi^+\pi^+\pi^-$  using a candidate driven vertex algorithm[8], and then we combined the  $\Xi_c^0$  candidate with an additional pion from the primary vertex to search for the  $\Xi_c^{*+}$  state<sup>1</sup>. The  $\Lambda$  and  $\bar{K}^0$  were reconstructed through their decays  $\Lambda \rightarrow p\pi^-$  and  $\bar{K}^0 \rightarrow K_S^0 \rightarrow \pi^+\pi^-$ , respectively. In each case, a pair of oppositely charged

---

<sup>1</sup>To search for the  $\Xi_c^*$  states, we studied various decay modes, including all previously observed ones, of the  $\Xi_c^0$  and  $\Xi_c^+$  baryons:  $p + X$ ,  $\Lambda + X$ ,  $\Xi^- + X$ ,  $\Sigma^+ + X$ , and  $\Omega^- + X$ . The  $\Lambda\bar{K}^0\pi^+\pi^-$  and  $\Lambda K^-\pi^+\pi^+\pi^-$  decay modes of the  $\Xi_c^0$  were selected to measure the  $\Xi_c^{*+}$  mass because only they exhibit statistically significant signals for either the  $\Xi_c^{*+}$  or  $\Xi_c^{*0}$  states.

tracks was required to originate from a common vertex. In the  $\Lambda$  reconstruction, we identified the higher momentum track as the proton candidate and required it to be consistent with a proton Čerenkov hypothesis. No particle identification requirement was used for the daughter pion tracks of the  $K_S^0$  candidate. The reconstructed mass of the  $\Lambda$  ( $K_S^0$ ) candidate was required to be within  $8.0 \text{ MeV}/c^2$  of the nominal  $\Lambda$  ( $K_S^0$ ) mass[9]. The charged daughter tracks of the  $\Xi_c^0$  decay had to be reconstructed in both the SSD and PWC systems. The kaon track was required to be consistent with a kaon Čerenkov hypothesis and the pion was required to be *inconsistent* with the hypothesis of an electron, kaon, or proton.

All charm daughter tracks were required to extrapolate back to a single point (the secondary vertex) with a confidence level greater than 1%. The primary vertex was reconstructed by intersecting the momentum vector of the  $\Xi_c^0$  candidate with the remaining SSD tracks and by requiring the confidence level to be greater than 1%. The primary vertex was constrained to be within the target volume and to be upstream of the secondary vertex. The primary and secondary vertices were required to satisfy two isolation criteria. The first isolation estimator (the primary vertex isolation cut) was the confidence level of the hypothesis that a track assigned to the secondary vertex be consistent with being in the primary vertex. The other estimator (the secondary decay vertex isolation cut) was the confidence level that any track in the event not already assigned in either vertex came from the secondary vertex. In this analysis, we required these two vertex isolation estimators to be less than 80% and 1%, respectively. No clear signal was observed in either the  $\Lambda K_S^0 \pi^+ \pi^-$  or the  $\Lambda K^- \pi^+ \pi^+ \pi^-$  invariant mass spectrum due to the large combinatoric background.

To search further, we looked for  $\Xi_c^0$ 's resulting from the production of  $\Xi_c^{*+}$ 's followed by decay to the  $\Xi_c^0$  through a pion emission. Correlation of this kind can be extremely helpful in overcoming combinatoric background. Each combination of  $\Lambda K_S^0 \pi^+ \pi^-$  or  $\Lambda K^- \pi^+ \pi^+ \pi^-$ , satisfying the selection criteria described above, was combined with each  $\pi^+$  track in the primary vertex to search for a higher mass state. The additional pion track was required to be consistent with a Čerenkov pion

hypothesis. For each  $\Xi_c^0\pi^+$  combination, the mass difference,  $\Delta M = M(\Xi_c^0\pi^+) - M(\Xi_c^0)$ , was calculated. In Figure 1-(a) we presented a scatter plot of the mass difference  $\Delta M$  versus the invariant mass of the  $\Xi_c^0$  candidate. The signal events are clustered within the small box of the plot. The scatter plot was fit to a two dimensional Gaussian signal, with fixed widths of  $2.5 \text{ MeV}/c^2$  and  $12.0 \text{ MeV}/c^2$  for the mass difference and the  $\Xi_c^0$  invariant mass respectively as determined by our Monte Carlo simulation, and a fully correlated two dimensional second order polynomial background using a  $\chi^2$  method. The  $\Xi_c^0$  mass and the mass difference were found to be  $2473.8 \pm 3.4 \text{ MeV}/c^2$  and  $177.2 \pm 0.5 \text{ MeV}/c^2$  in the fit. The statistical significance ( $S/\sqrt{B}$ ) of the signal was found to be about 6.7 based on  $40.7 \pm 8.2$  signal events above about 36 background events.

Selecting events within the two horizontal lines of the scatter plot, which satisfy a  $\Xi_c^0$  mass cut,  $|M(\Xi_c^0) - 2470.3| < 24.0 \text{ MeV}/c^2$ , we obtained the mass difference  $\Delta M$  distribution shown in Figure 1-(b), which shows a clear enhancement around  $177 \text{ MeV}/c^2$ . The mass difference distribution was fit to a Gaussian signal and a second order polynomial background function using a maximum likelihood method. A total of  $47.3 \pm 11.1$  signal events above the background was found in the fit with a mass difference of  $177.1 \pm 0.5 \text{ MeV}/c^2$  and a signal width<sup>2</sup> of  $2.0 \pm 0.4 \text{ MeV}/c^2$ .

On the other hand, the two vertical lines of the scatter plot correspond to a mass difference cut,  $|M(\Xi_c^0\pi^+) - M(\Xi_c^0) - 177.1| < 4.0 \text{ MeV}/c^2$ , around the observed ( $\Xi_c^0\pi^+$ ) state. Selecting only candidates inside this region, the invariant mass distribution of the  $\Xi_c^0$  candidate shown in Figure 1-(c) was obtained, which shows a clear signal around  $2470 \text{ MeV}/c^2$ . The invariant mass distribution was fit to a Gaussian signal, with a fixed width of  $12 \text{ MeV}/c^2$  as determined by Monte Carlo simulation, and a second order polynomial background using a maximum likelihood

---

<sup>2</sup>Theoretical estimations of the intrinsic width of the  $\Xi_c^{*+}$  state are in the range of a few  $\text{MeV}/c^2$  [1] and the CLEO collaboration determined the width to be less than  $3.1 \text{ MeV}/c^2$  at 90% confidence level[5]. Our signal width was found to be consistent with our detector resolution for a zero width particle.

method. We found  $45.5 \pm 9.7$  signal events above the background and determined the  $\Xi_c^0$  mass to be  $2471.8 \pm 3.6$  MeV/ $c^2$  from the fit. The value is in excellent agreement with the current world average of the  $\Xi_c^0$  mass[9]. The number of signal events found in the  $\Xi_c^0$  invariant mass distribution agrees well with the excess yield in the mass difference distribution and the fit to the two dimensional scatter plot. We, therefore, believe that the signals in the mass difference and the  $\Xi_c^0$  invariant mass distributions are strongly correlated and originate from a higher mass state ( $\Xi_c^{*+}$ ) decaying to  $\Xi_c^0\pi^+$ .

Figure 2-(a) shows a scatter plot of the *wrong sign* mass difference ( $M(\Xi_c^0\pi^-) - M(\Xi_c^0)$ ) versus the invariant mass of the  $\Xi_c^0$  candidate, where the  $\Xi_c^0$  candidate was selected using the identical analysis cuts discussed above but combined with each  $\pi^-$  track in the primary vertex. No significant enhancement around the signal region appears. Only  $1.5 \pm 4.4$  signal events over about 37 background events were found by the two dimensional fit described above. The wrong sign mass difference distribution (shown in Figure 2-(b)) and the invariant mass distribution of the  $\Xi_c^0$  candidate (shown in Figure 2-(c)) do not show any significant enhancement around the signal region. A fit to a Gaussian signal and a second order polynomial background function yielded only  $0.3 \pm 0.1$  signal events in the mass difference distribution and  $1.1 \pm 1.8$  signal events in the  $\Xi_c^0$  invariant mass distribution.

We split the mass difference distribution and the  $\Xi_c^0$  invariant mass distribution shown in Figure 1 into the two decay modes. Figure 3-(a) and (b) show the mass difference distributions respectively for the  $\Lambda K^- \pi^+ \pi^+ \pi^-$  and  $\Lambda K_S^0 \pi^+ \pi^-$  decay modes of the  $\Xi_c^0$  baryon, showing clear signal indications in both decay channels. Fits to a Gaussian signal and a second order polynomial background yielded  $\Delta M = 177.5 \pm 0.6$  MeV/ $c^2$  and  $26.5 \pm 8.0$  signal events in the  $\Lambda K^- \pi^+ \pi^+ \pi^-$  decay mode, and  $\Delta M = 176.6 \pm 0.7$  MeV/ $c^2$  and  $19.8 \pm 7.8$  signal events in the  $\Lambda K_S^0 \pi^+ \pi^-$  decay mode. Figure 3-(c) and (d) show the  $\Xi_c^0$  invariant mass distributions separately for the  $\Lambda K^- \pi^+ \pi^+ \pi^-$  and  $\Lambda K_S^0 \pi^+ \pi^-$  decay modes. Each invariant mass distribution was fit to a Gaussian signal, with a fixed width of 12.0 MeV/ $c^2$ , and a

second order polynomial background. The fit yielded  $26.3 \pm 7.1$  signal events in the  $\Lambda K^- \pi^+ \pi^+ \pi^-$  decay mode with the  $\Xi_c^0$  mass of  $2471.8 \pm 4.4$  MeV/ $c^2$  and  $18.9 \pm 6.6$  signal events in the  $\Lambda K_S^0 \pi^+ \pi^-$  decay mode with the mass of  $2471.7 \pm 6.0$  MeV/ $c^2$ .

A careful and detailed study of the stability and behavior of the  $\Xi_c^{*+}$  and  $\Xi_c^0$  signals was performed using several sets of analysis cuts. In the study we checked the signal shape and event yield, the mass difference and the  $\Xi_c^0$  mass, and compared them with Monte Carlo predictions. We found that our signals are not biased by the choice of analysis cuts and that the evolution of the signal event yields as a function of the analysis cuts is well reproduced by the Monte Carlo.

Systematic errors in the mass difference and the  $\Xi_c^0$  mass measurements were estimated by two independent methods: the disjoint sample analysis and variations in the fitting procedure. In the disjoint sample analysis, we first split our data into two statistically independent subsamples and employed a slight variation of the *S-factor* method proposed by the Particle Data Group [9] to separate true systematic variations from statistical fluctuations. The data were split into two subsamples depending on the momentum, charge, decay mode, run periods, and analysis cuts. The data were split into two subsamples of approximately the same number of signal events by adjusting the cut parameter in question, while all the other cuts were fixed at a reference value. The mass difference or the  $\Xi_c^0$  mass was evaluated for each of the statistically independent subsamples and a *scaled variance* was calculated; the *split sample* variance was defined as the difference between the reported statistical variance and the scaled variance when the scaled variance was larger than the statistical variance. In the split sample analysis, we noticed that the mass difference can be shifted by 1.1 MeV/ $c^2$  at the most and the  $\Xi_c^0$  mass by 2.6 MeV/ $c^2$ .

Additional systematic effects related to variations in the fitting procedure (the bin size, fit method, and background model) were also evaluated. First, we studied the mass difference (the  $\Xi_c^0$  invariant mass) distribution for several different bin sizes, from 1 to 4 (from 8 to 12) MeV/ $c^2$ , and found that the mass difference

(the  $\Xi_c^0$  mass) measurement is not affected by the choice of histogram bin size. Second, to estimate the effect of the fit method we compared the results obtained by a maximum likelihood fit and a  $\chi^2$  fit using the same fit function, and found no significant difference between the two fit methods. We also investigated the effect of fixing the signal Gaussian width in the fit, and found no significant shift in the mass difference and about  $0.4 \text{ MeV}/c^2$  shift in the  $\Xi_c^0$  mass. Third, we carefully studied possible systematic effects originating from the background model. For this study, we obtained the parameters of the background function<sup>3</sup> by fitting the mass difference (the  $\Xi_c^0$  invariant mass) distribution obtained by wrong-sign combination events and the one obtained from the  $\Xi_c^0$  ( $\Xi_c^{*+}$ ) sideband events, and used them as a *true* background distribution in fitting the mass difference ( $\Xi_c^0$  invariant mass) distribution. We also studied the mass difference (the  $\Xi_c^0$  invariant mass) distribution using a *background subtraction* method, where two different background distributions were used: the one obtained from wrong-sign combinations and the other obtained from the  $\Xi_c^0$  ( $\Xi_c^{*+}$ ) sideband events. We found no meaningful fluctuation in the mass difference measurement resulted from the background model and about  $1.3 \text{ MeV}/c^2$  systematic shift in the  $\Xi_c^0$  mass. We found no significant systematic shift in the mass difference measurement and about  $1.4 \text{ MeV}/c^2$  systematic fluctuation in the  $\Xi_c^0$  mass measurement related to variations in the fitting procedure.

Combining all source of systematics in quadrature, we determined the total systematic error in the mass difference measurement to be  $1.1 \text{ MeV}/c^2$  and the one in the  $\Xi_c^0$  mass measurement to be  $3.0 \text{ MeV}/c^2$ .

We assigned a conservative systematic error of  $1.1 \text{ MeV}/c^2$  in the mass difference measurement and determined the mass difference to be  $177.1 \pm 0.5 \pm 1.1 \text{ MeV}/c^2$ ,

---

<sup>3</sup>We parameterized the background in the mass difference distribution using a second order polynomial and two different threshold functions:  $A \cdot (\Delta M - m_\pi)^B \cdot \exp(-C \cdot (\Delta M - m_\pi))$  and  $A \cdot (\Delta M - m_\pi)^{0.5} + B \cdot (\Delta M - m_\pi)^{1.5} + C \cdot (\Delta M - m_\pi)^{2.5}$ , where  $A$ ,  $B$ , and  $C$  are free fit parameters,  $\Delta M$  is the mass difference, and  $m_\pi$  is the pion mass. These two threshold functions were formulated to vanish at the pion emission threshold. However, we used only a second order polynomial to parameterize the background in the  $\Xi_c^0$  invariant mass distribution.

where the first error is statistical and the second is systematic. Our measurement is about  $1.7\sigma$  higher than the recent CLEO measurement,  $174.3 \pm 0.5 \pm 1.0$  MeV/ $c^2$  [5]. We conclude that we have observed the same excited state, the  $\Xi_c^{*+}$ , of the  $\Xi_c^+$  baryon as the CLEO collaboration. We quoted a conservative systematic error of 3.0 MeV/ $c^2$  in the  $\Xi_c^0$  mass measurement and determined the  $\Xi_c^0$  mass to be  $2471.8 \pm 3.6 \pm 3.0$  MeV/ $c^2$ . Our measurement of the  $\Xi_c^0$  mass is in excellent agreement with the current world average[9], while it is about  $1.7\sigma$  higher than our previous measurement[7] determined using the  $\Xi_c^0 \rightarrow \Xi^- \pi^+$  decay mode. We reanalyzed the  $\Xi_c^0 \rightarrow \Xi^- \pi^+$  decay mode after removing a minor bias found in our previous analysis. Using the identical analysis criteria discussed in our previous paper[7], we obtained the  $\Xi^- \pi^+$  invariant mass distribution shown in Figure 4. Fitting to a Gaussian signal and a second order polynomial background, we found the  $\Xi_c^0$  signal yield and mass to be  $39.8 \pm 10.9$  events and  $2467.5 \pm 4.3 \pm 5.5$  MeV/ $c^2$ , respectively, which are all consistent with our previous measurements. However, the statistical error was determined to be larger than that in our previous measurement mainly due to the worse signal-to-noise ratio. The systematic error was also found to be underestimated in our previous analysis and was determined to be 5.5 MeV/ $c^2$  using almost identical techniques discussed in this paper. Combining the two independent measurements, we determined the  $\Xi_c^0$  mass to be  $2470.0 \pm 2.8 \pm 2.6$  MeV/ $c^2$ .

In conclusion, we confirm the existence of the  $\Xi_c^{*+}$  state decaying into  $\Xi_c^0 \pi^+$ . We have identified two previously unobserved decay modes of the  $\Xi_c^0$  baryon:  $\Lambda \bar{K}^0 \pi^+ \pi^-$  and  $\Lambda K^- \pi^+ \pi^+ \pi^-$ . We have measured the mass difference  $M(\Xi_c^{*+}) - M(\Xi_c^0)$  to be  $177.1 \pm 0.5 \pm 1.1$  MeV/ $c^2$  and the  $\Xi_c^0$  mass to be  $2470.0 \pm 2.8 \pm 2.6$  MeV/ $c^2$ .

We wish to acknowledge the assistance of the staffs of the Fermi National Accelerator Laboratory, the INFN of Italy, and the physics departments of the collaborating institutions. This research was supported in part by the National Science Foundation, the U.S. Department of Energy, the Italian Istituto Nazionale di Fisica Nucleare and Ministero dell'Università e della Ricerca Scientifica e Tecnologica, and the Korean Science and Engineering Foundation.

## References

- [a] Present address: Fermilab, Batavia, IL 60510, USA.
  - [b] Present address: University of Maryland, College Park, MD 20742, USA.
  - [c] Present address: University of South Carolina, Columbia, SC 29208, USA.
  - [d] Present address: Vanderbilt University, Nashville, TN 37235, USA.
  - [e] Present address: Enrico Fermi Institute, University of Chicago, Chicago, IL 60637, USA.
  - [f] Present address: Indiana University, Bloomington, IN 47405, USA.
  - [g] Present address: Syracuse University, Syracuse, NY 13244-1130, USA.
  - [h] Present address: University of Colorado, Boulder, CO 80309, USA.
  - [i] Present address: University of New York, Stony Brook, NY 11794, USA.
  - [j] Present address: AT&T, West Long Branch, NJ 07765, USA.
  - [k] Present address: Pohang Accelerator Laboratory, Pohang 790-784, Korea.
  - [l] Present address: Science Applications International Corporation, McLean, VA 22102, USA.
  - [m] Present address: Gamma Products Inc., Palos Hills, IL 60465, USA.
  - [n] Present address: Lucent Technologies, Lisle, IL 60532-3640, USA.
  - [o] Present address: University of Pittsburgh, Pittsburgh, PA 15260, USA.
  - [p] Present address: Brookhaven National Laboratory, Upton, NY 11793-5000, USA.
  - [q] Present address: KEK, National Laboratory for High Energy Physics, Tsukuba 305, Japan.
- [1] A. De Rújula, H. Georgi, and S. L. Glashow, *Phys. Rev.* D12, 147 (1975); K. Maltman and N. Isgur, *Phys. Rev.* D22, 1701 (1980); J. Richard and P. Taxil, *Phys. Lett.* B128, 453 (1983); C. Itoh *et al.*, *Phys. Rev.* D40, 3660 (1989); J. Körner and H. Siebert, *Ann. Rev. Nucl. Part. Sci.* 41, 511 (1991); R. Cutkosky and P. Geiger, *Phys. Rev.* D48, 1315 (1993); J. Rosner, *Phys. Rev.* D52, 6461 (1995).
  - [2] R. Werding *et al.*, Proceedings of the 27th International Conference on High Energy Physics (Edited by P.J. Bussey and I.G. Knowles), 1023 (1995).
  - [3] T.E. Coan *et al.*, CLEO CONF 97-29 and EPS 97-393 (1997).
  - [4] P. Avery *et al.*, *Phys. Rev. Lett.* 75, 4364 (1995).
  - [5] L. Gibbons *et al.*, *Phys. Rev. Lett.* 77, 810 (1996).
  - [6] G. Brandenburg *et al.*, CLEO CONF 97-17 and EPS 97-398 (1997).
  - [7] P. L. Frabetti *et al.*, *Phys. Rev. Lett.* 70, 2058 (1993).
  - [8] P. L. Frabetti *et al.*, *Nucl. Instru. & Meth.* A320, 519 (1992).
  - [9] R. M. Barnett *et al.*, *Phys. Rev.* D54, 1 (1996).

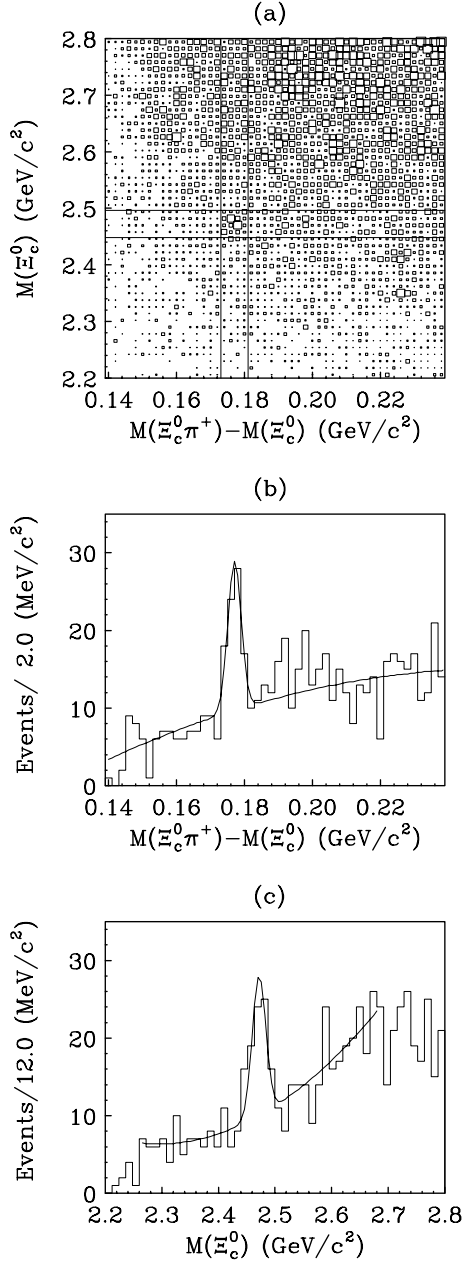


Figure 1: (a) shows a mass difference,  $M(\Xi_c^0 \pi^+) - M(\Xi_c^0)$ , versus  $M(\Xi_c^0)$  scatter plot for  $\Xi_c^0 \rightarrow \Lambda K_S^0 \pi^+ \pi^-$  and  $\Lambda K^- \pi^+ \pi^+ \pi^-$  combined: the mass difference is plotted on the x-axis and the invariant mass of  $\Xi_c^0$  candidate on the y-axis. (b) shows the mass difference distribution and (c) shows the invariant mass distribution of  $\Xi_c^0$  candidate. The curve in each histogram is the best fit discussed in the text.

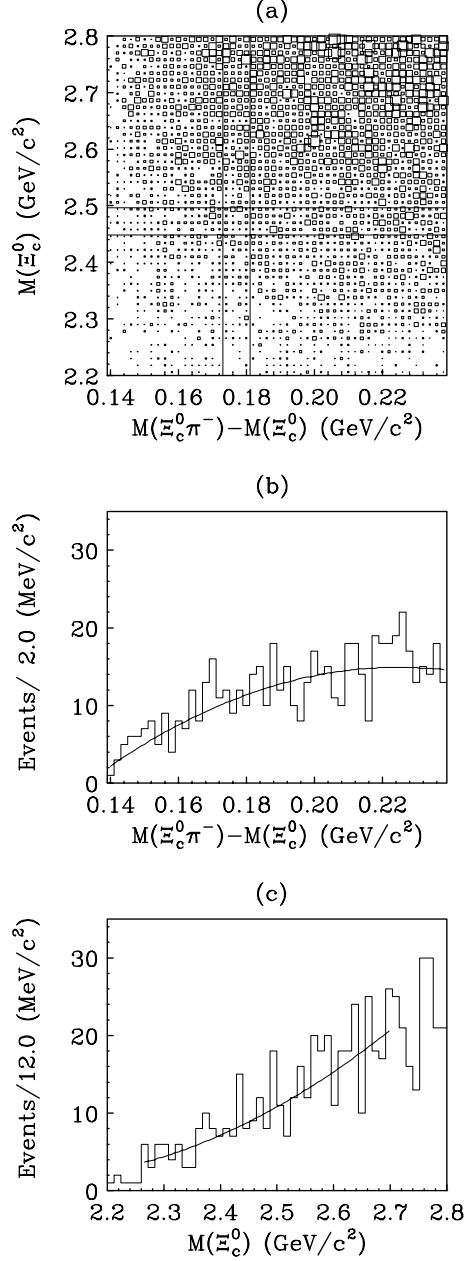


Figure 2: (a) shows a wrong sign mass difference,  $M(\Xi_c^0 \pi^-) - M(\Xi_c^0)$ , versus  $M(\Xi_c^0)$  scatter plot for  $\Xi_c^0 \rightarrow \Lambda K_S^0 \pi^+ \pi^-$  and  $\Lambda K^- \pi^+ \pi^+ \pi^-$  combined: the mass difference is plotted on the x-axis and the invariant mass of  $\Xi_c^0$  candidate on the y-axis. (b) shows the wrong sign mass difference distribution and (c) shows the invariant mass distribution of  $\Xi_c^0$  candidate. The curve in each histogram is the best fit discussed in the text.

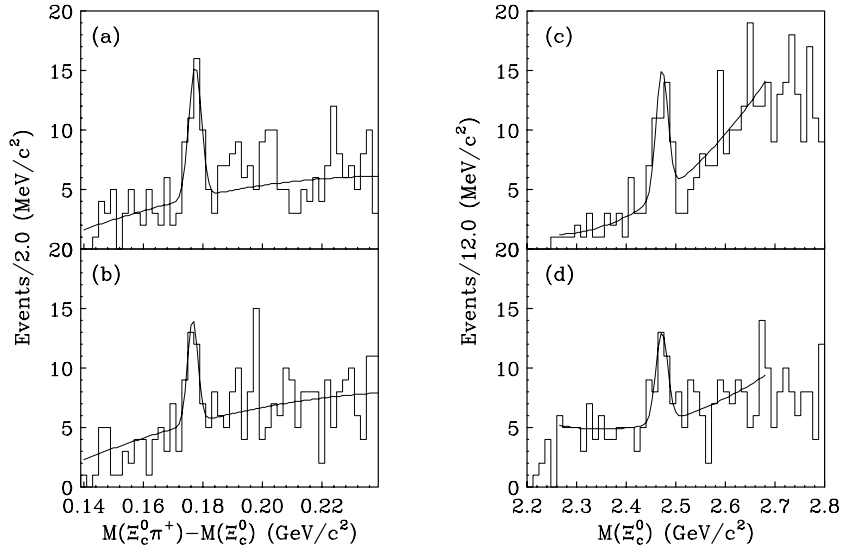


Figure 3: The mass difference distributions and the  $\Xi_c^0$  invariant mass distributions: (a) and (c) for  $\Xi_c^0 \rightarrow \Lambda K^- \pi^+ \pi^+ \pi^-$  decay, and (b) and (d) for  $\Xi_c^0 \rightarrow \Lambda K_S^0 \pi^+ \pi^-$  decay. The curve in each histogram is the best fit described in the text.

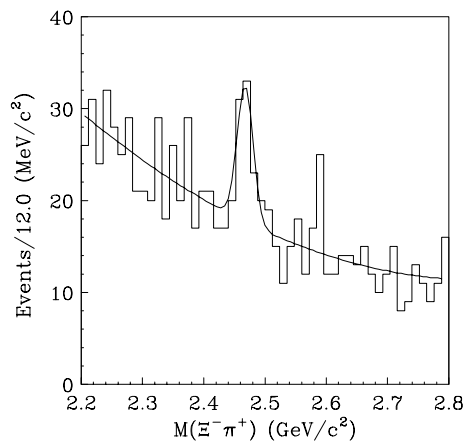


Figure 4: The  $\Xi^- \pi^+$  invariant mass distribution. The curve is the best fit described in the text.